Correlation Between Advanced Glycation End Products and Ultrasonographic Measurements of Cervico-Facial Skin Tissue

Anida-Maria Babtan , Claudia Feurdean , Stefan Cristian Vesa * , Octavia Sabin , Alexandra Roșioară , Sonia Irina Vlaicu , Antonia Eugenia Macarie , Aranka Ilea

Posted Date: 28 February 2026

doi: 10.20944/preprints202602.2001.v1

Keywords: skin; UV exposure; glycation products; high frequency ultrasound

Article

Correlation Between Advanced Glycation End Products and Ultrasonographic Measurements of Cervico-Facial Skin Tissue

Anida-Maria Babtan [1], Claudia Feurdean [1], Stefan Cristian Vesa [2,*], Octavia Sabin [2], Alexandra Rosioara [3], Sonia Irina Vlaicu [4], Antonia Eugenia Macarie [5] and Aranka Ilea [1]

[1] III[rd] Department-Oral Rehabilitation, Faculty of Dentistry, "Iuliu Haţieganu" University of Medicine and Pharmacy, 400347 Cluj-Napoca, Romania

[2] I[st] Department- Pharmacology, Toxicology and Clinical Pharmacology, Faculty of Medicine, "Iuliu Haţieganu" University of Medicine and Pharmacy, 400347 Cluj-Napoca, Romania

[3] III[rd] Department - Hygiene, Department of Community Medicine, "Iuliu Haţieganu" University of Medicine and Pharmacy, 400349 Cluj-Napoca, Romania
Research Center in Preventive Medicine, Health Promotion and Sustainable Development, "Iuliu Haţieganu" University of Medicine and Pharmacy, 400349 Cluj-Napoca, Romania

[4] IV[th] Department – Internal Medicine, Faculty of Medicine, "Iuliu Haţieganu" University of Medicine and Pharmacy, 400347 Cluj-Napoca, Romania

[5] V[th] Department – Geriatric-Gerontology, Faculty of Medicine, "Iuliu Haţieganu" University of Medicine and Pharmacy, 400347 Cluj-Napoca, Romania

* Correspondence: stefan.vesa@umfcluj.ro

Abstract

Background/Objectives: Advanced Glycation End Products (AGEs) are the end products of the Maillard reaction, derived from reduced sugars and proteins, lipids or DNA. AGEs accumulate in dermal collagen and elastin, causing several changes: skin stiffening and loss of elasticity, stimulation of inflammation and the result of accelerated photo- and chronological aging, manifested by skin yellowing, wrinkles, and dryness. High Frequency Ultrasound (HFU) offers precise and non-invasive assessments of structural and inflammatory changes in the skin: it measures the thickness of the epidermis and dermis, echogenicity and the hypoechoic band under the epidermis. The aim of the study is to correlate AGEs levels in biological fluids with ultrasonographic measurements of sun-exposed skin and non-sun-exposed tissue. **Methods**: Patients (N=113) were enrolled and demographic, clinical, and anthropometric measurements were recorded: age, gender, body mass index (BMI), waist circumference, and Fitzpatrick skin type. Venous blood, urine and salivary samples were harvested. The following AGEs were assessed in biological fluids (plasma, saliva, urine): Fructose-Lysine, Pyridine, Methyl-Glyoxal-H1, Carboxyethyl-lysine, Carboxymethyllysine, Arginine, Lysine. The tissue glycation process of collagen fibers was indirectly evaluated with a 22 MHz HFU ultrasound device (DUB cutis, Taberna Pro Medicum, Lüneburg, Germany)**.** The assessment was performed on sun-exposed skin (left zygomatic area) and on non-sun-exposed tissue (non-keratinized mucosa of the lower lip)**.** For the sun-exposed skin of the zygomatic area, including the epidermis, dermis, and subcutaneous tissue (hypodermis), tissue depth (thickness), pixel count (px), and density (automatic) were recorded. The non-sun-exposed tissue examined was the oral mucosa on the inner surface of the lower lip including the non-keratinized epithelium, lamina propria, and submucosa. **Results**: The study evidences a weak positive correlation between UV exposed dermis collagen and serum Pyr, salivary MG-H1, salivary Arg and salivary Lys. Between biofluid AGEs and the degree of pixelation of dermal collagen exposed to UV rays, we determined weak direct correlations with salivary MG-H1 and salivary CML. Significant indirect weak and medium correlations were found between dermal collagen density affected by UV exposure with serum CEL, Arg, Lys, weak direct correlation with salivary MG-H1 and salivary CML. Regarding the

 doi:10.20944/preprints202602.2001.v1

density of the dermis affected by UV exposure, we found a weak indirect correlation with salivary FruLys, MG-H1, CML and Lys . **Conclusions:** HFU ultrasound assessment revealed structural changes in the cervico-facial dermis, which were associated with increased AGEs, suggesting that glycation-induced tissue remodeling can be detected non-invasively. This data obtained might be the based for future studies on the clinical utility of the combined assessment of AGEs and skin changes by HFU as modern, rapid and non-invasive tools to identify patients at increased cardiovascular risk.

Keywords: skin; UV exposure; glycation products; high frequency ultrasound

1. Introduction

Health is defined as a state of physical, mental, and social well-being and not merely the absence of disease or infirmity [1]. The global population is continuously aging, and most adult patients experience the second stage of life accompanied by associated pathology and disability Although the decline in physiological resources is associated with the aging process, frailty brings with it an acceleration of the decline, and homeostasis mechanisms no longer react within appropriate parameters. However, in the presence of comorbidities, reduced physical activity, unbalanced dietary intake, and a precarious economic status, the risks of imbalance are higher.

Advanced Glycation End Products (AGEs) are the end products of the Maillard reaction, derived from reduced sugars and proteins, lipids or DNA [2]. In MS, chronic hyperglycemia and oxidative stress accelerate the generation of reactive dicarbonyls (e.g. methylglycoxal H1- MG) that are converted into AGEs [1,2]. AGEs such as carboxy-methyl-lysine (CML), carboxy-ethyl-lysine (CEL), fructose-lysine (Fru-Lys), pyridine (Pyr), arginine (Arg) are involved in tissue stiffening, inflammation through activation of the AGE receptor (RAGE) and induction of proinflammatory pathways NF κB, metaloproteinases and degradation of the extracellular tissue matrix [3].

Impact of AGEs on skin structure and function AGEs accumulate in dermal collagen and elastin, causing: skin stiffening and loss of elasticity through covalent bonds between collagen/elastin fibers [3], stimulation of inflammation through the RAGE → NF κB → MMP → extracellular matrix activation mechanism, and most clinically evident, the result of accelerated photo- and chronological aging, manifested by skin yellowing, wrinkles, and dryness. Studies have shown that skin levels of AGEs measured by autofluorescence are correlated with carotid intima-media thickness (a cardiovascular marker) and vascular stiffness [4]. AGEs measured by autofluorescence in type 1 diabetes are predictive of macro- and microangiopathic complications [5]. Cutaneous AGEs are valuable markers for vascular complications and respond to intensive glycemic management.

Regarding the ultrasound assessment of skin aging, High Frequency Ultrasound (HFU), where HFU ≥20MHz, offers precise and non-invasive assessments of structural and inflammatory changes in the skin: it measures the thickness of the epidermis and dermis, echogenicity and the hypoechoic band under the epidermis [6,7]. In MetS, HFU highlights thin epidermis, low cell density, thicker dermis in sun-exposed areas [6]. On the other hand, in autoimmune pathology, in atopic dermatitis, the hypoechoic band under the epidermis is thicker in lesions and present in apparently healthy areas, indicating chronic subclinical inflammation, known as metainflammation [7].

According to the latest research, HFU has become increasingly used in medical diagnosis, especially in dermatological oncology, where HFU is used in a predominant manner, because the examination of malignant pathology involves early diagnosis of neoplastic formations, the authors claim that HFU ensures the acquisition of essential and objective information regarding tumor depth, lateral extension, degree of vascularization [8]. HFU has the advantage of highlighting structural skin changes, which reflect the degradation given by the cross-linking of collagen fibers and skin aging through the consequent loss of elasticity. AGEs are represented by compounds of exogenous or endogenous origin resulting from the non-enzymatic glycation of protein and carbohydrate groups, and their role in the occurrence and chronicity of systemic inflammation is under continuous

 doi:10.20944/preprints202602.2001.v1

research. Moreover, their effect on collagen fibers also has a visible component, which can be quantified by HFU and autofluorescence [8].

Another area explored by HFU is the evaluation of inflammatory skin diseases, such as differentiating between the inflammatory and sclerotic stages of scleroderma, by increasing collagen deposits, which are visible by HFU ultrasound [9]. In aesthetic medicine, HFU has applicability in the injection of dermal fillers, by measuring the depth before the procedure, but also for monitoring the results, being also used in monitoring anti-cellulite therapies, and the formation of postoperative scars. Other applications of HFU are in examining the skin and determining the degree of tissue aging, by monitoring the arrangement of collagen and elastin fibers, the degree of hydration, the presence and characteristics of the hypoechoic subepidermal band, which tends to change with age [10].

HFU also has applicability in cosmetology pharmacology, in industry and anti-aging therapy (e.g. chemical peeling, platelet-rich-plasma injection), HFU quantifies the effectiveness of treatments through changes in the epidermis and dermal parameters [11]. Thus, HFU allows clear monitoring of inflammation and tissue response to interventions in MetS and skin aging. HFU is a promising tool for the early detection of inflammation and changes induced by chronic systemic pathology, such as that generating AGEs in the skin structure, but also collagen aging correlated with predisposing factors – tobacco use, exposure to ultraviolet rays, consumption of foods from the Western Diet category, cooked at high temperatures and short cooking time.

Taking into account what was presented in the introductory part, the aim of the study is to compare AGEs in biological fluids with ultrasonographic changes induced by AGEs visible through HFU, in sun-exposed and non-exposed skin. The aim of the study is to correlate AGEs levels in biological fluids with ultrasonographic measurements of sun-exposed skin and non-sun-exposed tissue.

2. Materials and Methods

This study is analytical, observational, cross-sectional. Patients (N = 113) were recruited from the Departments of Oral Rehabilitation and Oral Prosthetics (Faculty of Dentistry, "Iuliu Haţieganu" University of Medicine and Pharmacy) and from the Regional Diabetes Center in Cluj-Napoca, Romania, between 2018 and 2019.

Inclusion criteria were patients over 18 years of age who required clinical examination and diagnosis of the oral cavity and diagnosis, associated or not with dental treatment needs. Exclusion criteria were patients weighing more than 150 kg (which exceeded the assessment capacity of the measuring device) and patients with skin and/or oral mucosa lesions or vascular anomalies. This study was approved by the University Ethics Board, no. 93/08.03.2017. Written informed consent was obtained from all subjects, according to the Declaration of Helsinki of the World Medical Association, revised in 2000, in Edinburgh.

Study Protocol

Clinical Evaluation

Patients were asked to report to the Oral Rehabilitation Department at 7:30 a.m. for enrollment, where they were asked to complete written informed consent regarding the procedures that would follow after inclusion in the clinical study. Demographic, clinical, and anthropometric measurements were recorded: age, gender, body mass index (BMI), waist circumference, and Fitzpatrick skin type (Figure 1). Venous blood was collected from the upper arm of the included subjects and collected in sterile osmotic tubes, centrifuged at 4000 rpm/14 min, plasma and serum were divided and stored in 100, 200, 500 µl samples, in sterile criotubes. Urine samples were brought by patients in sterile tubes. Urine was divided and stored in 100, 200, 500 µl samples, in sterile criotubes.

Saliva samples were harvested by using sterile cotton swabs, which were held by the patients in the oral cavity for three minutes, after putting them in sterile tubes (Salivette®, Sarstedt, AG & Co.,

 doi:10.20944/preprints202602.2001.v1

Numbrecht, Germany) (Image 1). Saliva was centrifuged (1450 rpm/2min) and sampled in 100, 200, 500 µl sterile crio-microtubes. The following AGEs were assessed in biological fluids (plasma, saliva, urine): FruLys, Pyr, MG-H1, CEL, CML, Arg, Lys.

Fitzpatrick skin phototype	Characteristics	Ultraviolet sensitivity
I	Pale, clear white skin, blue/green eyes, blonde/red hair	Always burns, does not tan
II	Fair skin, blonde hair, blue/ green eyes	Easily burns, tans poorly
III	Cream, dark white skin, light brown hair, brown/green eyes	Sometimes burns, tans after initial burn
IV	Light brown/olive skin, brown/dark hair and eyes colour	Rarely burns, easily tans
V	Moderate/dark brown skin and eyes colour	Extremely rarely burns, easily tans
VI	Dark brown/black skin, hair and eyes	Never burns, deep skin pigmentation

Figure 1. Types of skin phototype according to the Fitzpatrick classification**.**

Image 1. Saliva harvesting kit (Salivette®, Sarstedt, AG & Co., Numbrecht, Germany).

Ultrasound Evaluation

The tissue glycation process of collagen fibers was indirectly evaluated with a 22 MHz HFU ultrasound device (DUB cutis, Taberna Pro Medicum, Lüneburg, Germany), with a signal penetration depth of 8 mm, axial resolution of 57 µm at 22 MHz. Measurements were performed with the windows covered with curtains (to avoid UV-induced evaluation errors), at an ambient temperature of 25 °C. The ultrasound probe was used as a transmission medium for both the ultrasound gel (applied to the examined surface) and the water introduced into the HFU probe and covered with a thin transparent membrane. Ultrasound images were acquired in B-scan and A-scan viewing modes. The assessment was performed on sun-exposed skin (left zygomatic area) and on non-sun-exposed tissue (non-keratinized mucosa of the lower lip). Before measurements were taken, patients were asked to remove moisturizer/face concealer, if present. The transducer was placed parallel with and without pressure on both the zygomatic and inner lower lip regions after gel application.

Ultrasound measurements were performed by two operators (AMB and SCV). Each assessment was performed three times by each operator. For each site examined, HFU was performed at three different points (mesial, central and distal). The final value was the sum of the values. When differences in values were identified, the respective measurement was repeated by the two operators, reaching mutual agreement between the examiners. Intra-rater reliability was assessed for epidermal depth measurements. The correlation coefficient was 0.787, indicating good reliability. Inter-rater

 doi:10.20944/preprints202602.2001.v1

reliability was assessed for epidermal depth measurements using Cohen's kappa coefficient, which revealed a k of 0.881. For the sun-exposed skin of the zygomatic area, including the epidermis, dermis, and subcutaneous tissue (hypodermis), tissue depth (thickness), pixel count (px), and density (automatic) were recorded (Image 2). The non-sun-exposed tissue examined was the oral mucosa on the inner surface of the lower lip including the non-keratinized epithelium, lamina propria, and submucosa (Image 3). The following parameters were recorded: depth (thickness), pixel count (px), and density.

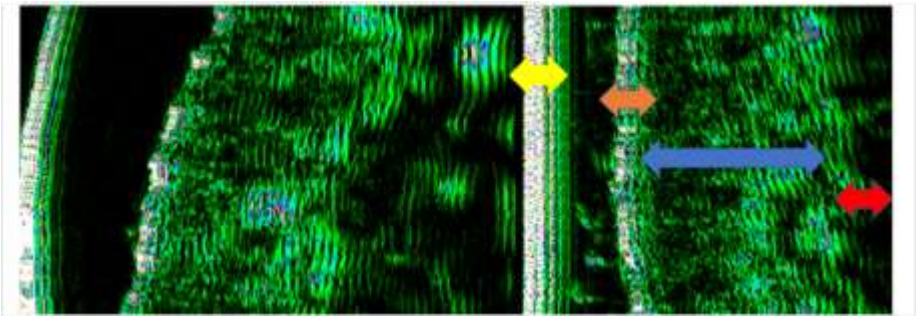

Image 2. HFU ultrasound assessment (DUB® cutis, Taberna Pro Medicum) of the lower lip structures, images are exported as pixels in order to highlight tissue density (white and blue – very dense, green – dense, black – very low density or muscular structure) yellow arrow – transducer membrane, Orange arrow – hyperpixelated epidermis, Blue arrow – dermis, Red arrow – hypopixelated hypodermis.

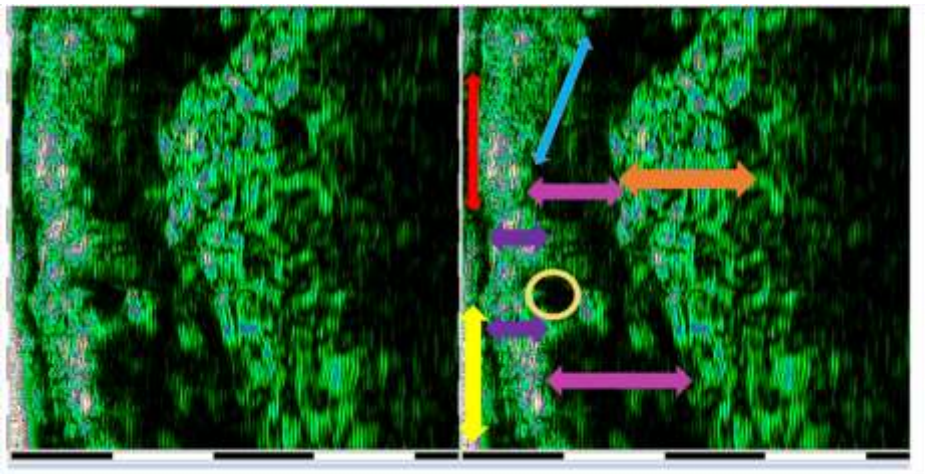

Image 3. HFU ultrasound assessment (DUB® cutis, Taberna Pro Medicum) of the lower lip structures**.** yellow arrow - superficial layer of non-keratinized squamous epithelium red arrow - spinous and basal layers of non-keratinized squamous epithelium purple arrow - papillary and reticular layers of the lamina propria mucosae orange arrow - tela submucosa yellow circle - minor salivary gland pink arrow - orbicularis oris muscle.

Statistical Analysis

Statistical analysis was performed using the statistical software MedCalc version 19.2.1 (MedCalc Software Ltd., Ostend, Belgium; https://www.medcalc.org; 2020). Quantitative variables were tested for normality of distribution using the Shapiro-Wilk test and were expressed as median and 25th-75th percentiles. Quantitative data were described using median and 25-75 percentiles. Qualitative data were characterized by frequency and percentage. Correlations between variables were performed using the Spearman coefficient. A p value <0.05 was considered statistically significant.

3. Results

 doi:10.20944/preprints202602.2001.v1

Data regarding anthropometric, high frequency ultrasound evaluation parameters and AGEs in biofluids (saliva, plasma, serum, urine) are shown in Table 1.

Table 1. Biochemical and ultrasound assessment in included subjects.

Characteristic		N (=113)
Age		52 (36; 60)
Gender	Male	37 (32.7%)
	Female	76 (67.3%)
Epidermis depth		281 (243; 325)
Epidermis nr pixels		5361.5 (4062; 4760)
Epidermis density		63.31 (47.61; 82.69)
Epidermis density %		26.1300 (19.8; 32.7)
Uv dermis exposure damage depth uv aged dermis		547 (394.5; 684)
Uv dermis exposure damage nr pixels		8806 (6312.5; 10979)
Uv dermis exposure damage density		9.8 (5.4; 17.5)
Uv dermis exposure damage density %		8.4 (6; 14.6)
Dermis Depth		1450 (1269.5; 1680)
Dermis nr pixels		23681 (20185; 27083.5)
Dermis density %		19.8 (15.2; 26.2)
Sc tissue depth		1594 (1094; 2164)
Sc tissue nr pixels		25320 (18000; 33201)
Sc tissue density		7.5 (5.2; 12.1)
plasma FruLys [µg/ml]		267 (146.7; 423.2)
plasma Pyr [ng/ml]		28.3 (24.9; 28.9)
plasma MG-H1 [ng/ml]		33.1 (31.3; 36.1)
plasma CEL [ng/ml]		13.2 (12.9; 13.4)
plasma CML [ng/ml]		49.1 (46.2; 51.8)
plasma Arg [µg/ml]		3.6 (2.6; 6.5)
plasma Lys [µg/ml]		6 (5.2; 7.2)
serum FruLys [µg/ml]		293.5 (205; 380.9)
serum Pyr [ng/ml]		28.4 (25.2; 29)
serum MG-H1 [ng/ml]		33.2 (31.3; 36.3)
serum CEL [ng/ml]		13.3 (12.8; 13.6)
serum CML [ng/ml]		46.9 (44.1; 49)
serum Arg [µg/ml]		5.4 (4.1; 7)
serum Lys [µg/ml]		6.4 (5.7; 7.6)
urine FruLys [µg/mg Kreatinin]		3.2 (2.46; 5.3)
urine Pyr [µg/mg Kreatinin]		0.11 (0.07; 0.18)
urine MG-H1 [µg/mg Kreatinin]		3.2 (2.1; 5.1)
urine CEL [µg/mg Kreatinin]		0.3 (0.22; 0.38)
urine CML [µg/mg Kreatinin]		1.4 (1.1; 2.1)
urine Arg [µg/mg Kreatinin]		2.2 (1.6; 2.9)
urine Lys [µg/mg Kreatinin]		8.1 (4.9; 14.5)
saliva FruLys [ng/ml]		21.9 (21; 24.3)
saliva Pyr [ng/ml]		1.7 (1.6; 1.7)
saliva MG-H1 [ng/ml]		3 (2.5; 4.2715)
saliva CEL [ng/ml]		1.1 (1; 1.3)
saliva CML [ng/ml]		3.9 (3.2; 4.8)
saliva Arg [µg/ml]		0.49 (0.24; 0.83)
saliva Lys [µg/ml]		0.59 (0.26; 0.89)

*px – pixels; UV – ultraviolet; sc – subcutaneous tissue.

 doi:10.20944/preprints202602.2001.v1

We determined the existence of a weak direct correlation between plasma MG-H1 and epidermal thickness (r=0.208), a weak indirect correlation between epidermal thickness and plasma Arg (r=-0.189), and a weak indirect correlation between epidermal depth and serum CEL (r=-0.248) (Table 2).

Table 2. Correlations between AGE types and epidermal thickness.

Variable	EPIDERMIS DEPTH (N=113)	
	R	p
plasma FruLys [µg/ml]	0.170	0.071
plasma Pyr [ng/ml]	-0.167	0.077
plasma MG-H1 [ng/ml]	0.208*	0.027
plasma CEL [ng/ml]	0.055	0.564
plasma CML [ng/ml]	0.181	0.055
plasma Arg [µg/ml]	-0.189*	0.045
plasma Lys [µg/ml]	-0.170	0.071
serum FruLys [µg/ml]	0.011	0.904
serum Pyr [ng/ml]	-0.128	0.177
serum MG-H1 [ng/ml]	-0.047	0.625
serum CEL [ng/ml]	-0.248**	0.008
serum CML [ng/ml]	-0.402**	0.000
serum Arg [µg/ml]	-0.089	0.349
serum Lys [µg/ml]	-0.138	0.145
saliva FruLys [ng/ml]	0.045	0.637
saliva Pyr [ng/ml]	0.051	0.593
saliva MG-H1 [ng/ml]	0.204*	0.030
saliva CEL [ng/ml]	-0.011	0.907
saliva Arg [µg/ml]	0.223*	0.018
saliva Lys [µg/ml]	0.115	0.224
urine FruLys [µg/mg Kreatinin]	0.048	0.612
urine Pyr [µg/mg Kreatinin]	0.034	0.725
urine MG-H1 [µg/mg Kreatinin]	0.109	0.250
urine CEL [µg/mg Kreatinin]	0.157	0.097
urine CML [µg/mg Kreatinin]	0.159	0.093
urine Arg [µg/mg Kreatinin]	0.212*	0.024
urine Lys [µg/mg Kreatinin]	-0.027	0.780

We also determined a weak positive correlation between epidermal density and salivary MG-H1 (r=0.204), a weak direct correlation between epidermal density and salivary Arg (r=0.223) (Table 3).

Table 3. Correlations between AGE types and epidermal density.

Variable	EPIDERMIS DENSITY (N=113)	
	r	p
plasma FruLys [µg/ml]	0.066	0.488
plasma Pyr [ng/ml]	-0.010	0.913
plasma MG-H1 [ng/ml]	-0.032	0.734
plasma CEL [ng/ml]	-0.056	0.554
plasma CML [ng/ml]	-0.045	0.639
plasma Arg [µg/ml]	0.006	0.949
plasma Lys [µg/ml]	-0.019	0.838
serum FruLys [µg/ml]	0.111	0.241

 doi:10.20944/preprints202602.2001.v1

serum Pyr [ng/ml]	-0.082	0.386
serum MG-H1 [ng/ml]	-0.003	0.972
serum CEL [ng/ml]	0.015	0.877
serum CML [ng/ml]	0.031	0.744
serum Arg [µg/ml]	0.000	0.999
serum Lys [µg/ml]	-0.004	0.962
saliva FruLys [ng/ml]	0.045	0.637
saliva Pyr [ng/ml]	0.051	0.593
saliva MG-H1 [ng/ml]	0.204*	0.030
saliva CEL [ng/ml]	-0.011	0.907
saliva Arg [µg/ml]	0.223*	0.018
saliva Lys [µg/ml]	0.115	0.224
urine FruLys [µg/mg Kreatinin]	0.018	0.852
urine Pyr [µg/mg Kreatinin]	-0.003	0.975
urine MG-H1 [µg/mg Kreatinin]	0.012	0.896
urine CEL [µg/mg Kreatinin]	0.086	0.366
urine CML [µg/mg Kreatinin]	0.160	0.091
urine Arg [µg/mg Kreatinin]	-0.007	0.937
urine Lys [µg/mg Kreatinin]	0.088	0.355

Regarding advanced glycation end products and dermal collagen affected by UV exposure, we established a weak positive correlation with serum Pyr (r=.227*), a weak direct correlation with salivary MG-H1 (r= 0.285**) and salivary CML (r=0.295). Also, weak direct correlations were determined between dermal affected by UV exposure and salivary Arg (r=0.207*), salivary Lys (r=0.200*). Indirect correlations were between dermal collagen affected by UV exposure and urinary MG-H1 (r=-0.194*), urinary CML (r=-0.252**) (Table 4).

Table 4. Correlations between types of AGEs and depth of dermal collagen affected by UV exposure.

Variable	UV DERMIS EXPOSURE DAMAGE DEPTH UV AGED DERMIS (N=113)	
	r	p
plasma FruLys [µg/ml]	-0.118	0.213
plasma Pyr [ng/ml]	0.125	0.188
plasma MG-H1 [ng/ml]	-0.052	0.585
plasma CEL [ng/ml]	0.145	0.126
plasma CML [ng/ml]	-0.065	0.492
plasma Arg [µg/ml]	0.091	0.337
plasma Lys [µg/ml]	0.151	0.110
serum FruLys [µg/ml]	-0.070	0.464
serum Pyr [ng/ml]	0.227*	0.016
serum MG-H1 [ng/ml]	-0.126	0.183
serum CEL [ng/ml]	0.015	0.877
serum CML [ng/ml]	-0.115	0.224
serum Arg [µg/ml]	-0.010	0.912
serum Lys [µg/ml]	0.071	0.453
saliva FruLys [ng/ml]	0.184	0.051
saliva Pyr [ng/ml]	0.026	0.787
saliva MG-H1 [ng/ml]	0.285**	0.002
saliva CEL [ng/ml]	0.039	0.685
saliva CML [ng/ml]	0.295**	0.001
saliva Arg [µg/ml]	0.207*	0.028

 doi:10.20944/preprints202602.2001.v1

saliva Lys [µg/ml]	0.200*	0.034
urine FruLys [µg/mg Kreatinin]	-0.035	0.710
urine Pyr [µg/mg Kreatinin]	-0.126	0.183
urine MG-H1 [µg/mg Kreatinin]	-0.194*	0.039
urine CEL [µg/mg Kreatinin]	-0.020	0.829
urine CML [µg/mg Kreatinin]	-0.252**	0.007
urine Arg [µg/mg Kreatinin]	-0.070	0.460
urine Lys [µg/mg Kreatinin]	0.064	0.498

Regarding the correlation between glycation end products in biofluids and the degree of pixelation of dermal collagen exposed to UV rays, we determined weak direct correlations with salivary MG-H1 (r=0.193*), salivary CML (r=0.227*), and weak indirect correlation with urinary CML (r=-0.240*) (Table 5).

Table 5. Correlations between types of AGEs and the degree of pixelation of dermal collagen affected by UV ray exposure.

Variable	UV DERMIS EXPOSURE DAMAGE NR PIXELS (N=113)	
	r	p
plasma FruLys [µg/ml]	-0.029	0.763
plasma Pyr [ng/ml]	0.063	0.509
plasma MG-H1 [ng/ml]	-0.075	0.432
plasma CEL [ng/ml]	0.112	0.238
plasma CML [ng/ml]	-0.048	0.614
plasma Arg [µg/ml]	0.042	0.659
plasma Lys [µg/ml]	0.106	0.263
serum FruLys [µg/ml]	-0.006	0.947
serum Pyr [ng/ml]	0.149	0.115
serum MG-H1 [ng/ml]	-0.079	0.406
serum CEL [ng/ml]	0.047	0.619
serum CML [ng/ml]	-0.032	0.738
serum Arg [µg/ml]	-0.032	0.733
serum Lys [µg/ml]	0.065	0.494
saliva FruLys [ng/ml]	0.104	0.272
saliva Pyr [ng/ml]	-0.007	0.942
saliva MG-H1 [ng/ml]	0.193*	0.041
saliva CEL [ng/ml]	0.018	0.851
saliva CML [ng/ml]	0.227*	0.016
saliva Arg [µg/ml]	0.115	0.226
saliva Lys [µg/ml]	0.123	0.193
urine FruLys [µg/mg Kreatinin]	-0.037	0.700
urine Pyr [µg/mg Kreatinin]	-0.114	0.229
urine MG-H1[µg/mg Kreatinin]	-0.168	0.075
urine CEL [µg/mg Kreatinin]	-0.030	0.753
urine CML [µg/mg Kreatinin]	-0.240*	0.011
urine Arg [µg/mg Kreatinin]	-0.072	0.452
urine Lys [µg/mg Kreatinin]	0.058	0.542

Significant correlations were found between dermal collagen density affected by UV exposure as follows – positive direct correlation with plasma FruLys (r=0.363), moderate indirect correlation with plasma Pyr (r=-0.417), moderate indirect correlation with plasma Arg (r=-0.456), moderate

 doi:10.20944/preprints202602.2001.v1

indirect correlation with plasma Lys (r=-0.394), strong indirect correlation with serum Pyr (r=-0.547), weak indirect correlation with serum CEL (r= -0.241), moderate indirect correlation with serum Arg (r=-0.369), weak indirect correlation with serum Lys (r=-0.270), weak direct correlation with salivary MG-H1 (r=0.193) and salivary CML (r=.227). At the urinary level, chelated dermal collagen was weakly indirectly correlated with CML (r=-0.240) (Table 6).

Table 6. Correlations between types of AGEs and the density of the dermis affected by UV exposure.

Variable	UV DERMIS EXPOSURE DAMAGE DENSITY (N=111)	
	r	p
plasma FruLys [µg/ml]	0.363**	0.000
plasma Pyr [ng/ml]	-0.417**	0.000
plasma MG-H1 [ng/ml]	-0.036	0.709
plasma CEL [ng/ml]	-0.054	0.576
plasma CML [ng/ml]	0.048	0.619
plasma Arg [µg/ml]	-0.456**	0.000
plasma Lys [µg/ml]	-0.394**	0.000
serum FruLys [µg/ml]	0.008	0.937
serum Pyr [ng/ml]	-0.547**	0.000
serum MG-H1 [ng/ml]	-0.093	0.332
serum CEL [ng/ml]	-0.241*	0.011
serum CML [ng/ml]	-0.140	0.143
serum Arg [µg/ml]	-0.369**	0.000
serum Lys [µg/ml]	-0.270**	0.004
saliva FruLys [ng/ml]	0.104	0.272
saliva Pyr [ng/ml]	-0.007	0.942
saliva MG-H1 [ng/ml]	0.193*	0.041
saliva CEL [ng/ml]	0.018	0.851
saliva CML [ng/ml]	0.227*	0.016
saliva Arg [µg/ml]	0.115	0.226
saliva Lys [µg/ml]	0.123	0.193
urine FruLys [µg/mg Kreatinin]	-0.037	0.700
urine Pyr [µg/mg Kreatinin]	-0.114	0.229
urine MG-H1 [µg/mg Kreatinin]	-0.168	0.075
urine CEL [µg/mg Kreatinin]	-0.030	0.753
urine CML [µg/mg Kreatinin]	-0.240*	0.011
urine Arg [µg/mg Kreatinin]	-0.072	0.452
urine Lys [µg/mg Kreatinin]	0.058	0.542

Regarding the density of the dermis affected by UV exposure, we found a moderate indirect correlation with salivary FruLys (r=-.0295), weak indirect with salivary MG-H1 (r=-0.170), weak indirect with salivary CML (r=-0.195) and weak indirect with salivary Lys (r=-0.233) (Table 7).

Table 7. Correlations between AGE types in biofluids and the density of dermal collagen affected by UV exposure.

Variable	UV DERMIS EXPOSURE DAMAGE DENSITY (N=111)	
	r	p
saliva FruLys [ng/ml]	-0.295**	0.002
saliva Pyr [ng/ml]	-0.006	0.951

 doi:10.20944/preprints202602.2001.v1

saliva MG-H1 [ng/ml]	-0.170*	0.075
saliva CEL [ng/ml]	-0.101	0.292
saliva CML [ng/ml]	-0.195*	0.041
saliva Arg [µg/ml]	-0.180	0.059
saliva Lys [µg/ml]	-0.233*	0.014
urine FruLys [µg/mg Kreatinin]	0.012	0.904
urine Pyr [µg/mg Kreatinin]	0.137	0.152
urine MG-H1 [µg/mg Kreatinin]	0.196*	0.039
urine CEL [µg/mg Kreatinin]	0.135	0.156
urine CML [µg/mg Kreatinin]	0.075	0.432
urine Arg [µg/mg Kreatinin]	0.432	0.744
urine Lys [µg/mg Kreatinin]	-0.073	0.445

Dermal depth was weakly positively correlated with salivary Lys (r=0.228), weakly indirectly correlated with plasma CML (r=-0.203), urinary Frulys (r=-0.216), urinary MG-H1 (r=-0.224), urinary CML (r=-0.186) (Table 8).

Table 8. Correlations between AGE types in biofluids and dermis depth.

Variable	DERMIS DEPTH N=113	
	r	p
plasma FruLys [µg/ml]	0.113	0.233
plasma Pyr [ng/ml]	-0.075	0.429
plasma MG-H1 [ng/ml]	-0.145	0.125
plasma CEL [ng/ml]	-0.086	0.364
Plasma CML	-0.203*	0.031
plasma Arg [µg/ml]	0.042	0.662
plasma Lys [µg/ml]	0.090	0.342
serum FruLys [µg/ml]	0.073	0.443
serum Pyr [ng/ml]	-0.017	0.861
serum MG-H1 [ng/ml]	-0.184	0.052
serum CEL [ng/ml]	-0.178	0.059
serum CML [ng/ml]	-0.145	0.126
serum Arg [µg/ml]	-0.071	0.458
serum Lys [µg/ml]	-0.044	0.644
saliva FruLys [ng/ml]	0.158	0.095
saliva Pyr [ng/ml]	0.013	0.890
saliva MG-H1 [ng/ml]	0.158	0.096
saliva CEL [ng/ml]	0.050	0.596
Saliva CML	0.0170	0.072
saliva Arg [µg/ml]	0.154	0.104
saliva Lys [µg/ml]	0.228*	0.015
urine FruLys [µg/mg Kreatinin]	-0.216*	0.022
urine Pyr [µg/mg Kreatinin]	-0.111	0.243
urine MG-H1 [µg/mg Kreatinin]	-0.224*	0.017
urine CEL [µg/mg Kreatinin]	-0.172	0.069
urine CML [µg/mg Kreatinin]	-0.186*	0.048
urine Arg [µg/mg Kreatinin]	-0.159	0.094
urine Lys [µg/mg Kreatinin]	0.042	0.660

 doi:10.20944/preprints202602.2001.v1

The degree of pixelation of dermal collagen was correlated with plasma FruLys – weak direct correlation (r=0.256), with serum CEL – weak indirect correlation (r=-0.221), urinary FruLys (r=-0.221) (Table 09).

Table 9. Correlations between AGE types in biofluids and the degree of pixelation of the dermis.

Variable	DERMIS nr pixels N=113	
	r	p
plasma FruLys [µg/ml]	0.256**	0.006
plasma Pyr [ng/ml]	-0.181	0.055
plasma MG-H1 [ng/ml]	-0.174	0.066
plasma CEL [ng/ml]	-0.123	0.194
Plasma CML	-0.177	0.061
plasma Arg [µg/ml]	-0.001	0.989
plasma Lys [µg/ml]	0.036	0.703
serum FruLys [µg/ml]	0.174	0.066
serum Pyr [ng/ml]	-0.159	0.092
serum MG-H1 [ng/ml]	-0.093	0.329
serum CEL [ng/ml]	-0.221*	0.019
serum CML [ng/ml]	0.005	0.957
serum Arg [µg/ml]	-0.077	0.420
serum Lys [µg/ml]	-0.033	0.033
saliva FruLys [ng/ml]	-0.004	0.968
saliva Pyr [ng/ml]	-0.014	0.880
saliva MG-H1 [ng/ml]	0.002	0.985
saliva CEL [ng/ml]	-0.012	0.896
Saliva CML	0.046	0.629
saliva Arg [µg/ml]	-0.021	0.826
saliva Lys [µg/ml]	0.077	0.418
urine FruLys [µg/mg Kreatinin]	-0.221*	0.019
urine Pyr [µg/mg Kreatinin]	-0.102	0.283
urine MG-H1 [µg/mg Kreatinin]	-0.180	0.057
urine CEL [µg/mg Kreatinin]	-0.179	0.058
urine CML [µg/mg Kreatinin]	-0.177	0.061
urine Arg [µg/mg Kreatinin]	-0.158	0.095
urine Lys [µg/mg Kreatinin]	0.038	0.690

Regarding dermal density and advanced glycation end products in biofluids, we found a weak direct correlation with serum FruLys (r=0.203) and urinary CEL (r=0.220), a weak indirect correlation with plasma Lys (r=-0.210) (Table 10).

Table 10. Correlations between AGEs types in biofluids and dermal density.

Variable	DERMIS density N=113	
	r	p
plasma FruLys [µg/ml]	0.098	0.304
plasma Pyr [ng/ml]	-0.066	0.489
plasma MG-H1 [ng/ml]	0.066	0.485
plasma CEL [ng/ml]	-0.089	0.350
Plasma CML	0.061	0.519
plasma Arg [µg/ml]	-0.109	0.250
plasma Lys [µg/ml]	-0.210*	0.026
serum FruLys [µg/ml]	0.203*	0.031

 doi:10.20944/preprints202602.2001.v1

serum Pyr [ng/ml]	-0.182	0.054
serum MG-H1 [ng/ml]	0.067	0.478
serum CEL [ng/ml]	-0.057	0.551
serum CML [ng/ml]	0.002	0.979
serum Arg [µg/ml]	-0.032	0.737
serum Lys [µg/ml]	-0.052	0.586
saliva FruLys [ng/ml]	-0.053	0.580
saliva Pyr [ng/ml]	0.112	0.236
saliva MG-H1 [ng/ml]	0.050	0.601
saliva CEL [ng/ml]	-0.086	0.365
Saliva CML [µg/ml]	0.057	0.549
saliva Arg [µg/ml]	-0.041	0.669
saliva Lys [µg/ml]	0.032	0.734
urine FruLys [µg/mg Kreatinin]	0.003	0.972
urine Pyr [µg/mg Kreatinin]	0.150	0.112
urine MG-H1 [µg/mg Kreatinin]	0.171	0.071
urine CEL [µg/mg Kreatinin]	0.220*	0.019
urine CML [µg/mg Kreatinin]	0.133	0.159
urine Arg [µg/mg Kreatinin]	0.131	0.168
urine Lys [µg/mg Kreatinin]	0.026	0.785

Subcutaneous tissue depth was weakly directly correlated with plasma MG-H1 (r=0.208), and weakly indirectly with serum CML (r=-.290) (Table 11).

Table 11. Correlations between AGE types in biofluids and subcutaneous tissue depth**.**

Variable	SC TISSUE DEPTH N=111	
	r	p
plasma FruLys [µg/ml]	0.046	0.635
plasma Pyr [ng/ml]	0.014	0.881
plasma MG-H1 [ng/ml]	0.208*	0.029
plasma CEL [ng/ml]	0.008	0.936
Plasma CML	0.135	0.158
plasma Arg [µg/ml]	0.043	0.651
plasma Lys [µg/ml]	0.132	0.166
serum FruLys [µg/ml]	-0.063	0.513
serum Pyr [ng/ml]	0.013	0.893
serum MG-H1 [ng/ml]	-0.111	0.248
serum CEL [ng/ml]	-0.062	0.520
serum CML [ng/ml]	-0.290**	0.002
serum Arg [µg/ml]	-0.118	0.217
serum Lys [µg/ml]	0.083	0.388

We found a weak direct correlation between the degree of subcutaneous tissue pixelation and plasma MG-H1 (r=0.201), weak indirect correlation with serum CML (r=-0.213) (Table 12).

Table 12. Correlations between AGE types in biofluids and the degree of subcutaneous tissue pixelation**.**

Variable	SC TISSUE NR PIXELS N=111	
	r	p
plasma FruLys [µg/ml]	0.134	0.162
plasma Pyr [ng/ml]	-0.049	0.613
plasma MG-H1 [ng/ml]	0.201*	0.035

 doi:10.20944/preprints202602.2001.v1

plasma CEL [ng/ml]	-0.035	0.712
Plasma CML	0.140	0.142
plasma Arg [µg/ml]	0.026	0.786
plasma Lys [µg/ml]	0.103	0.283
serum FruLys [µg/ml]	-0.007	0.942
serum Pyr [ng/ml]	-0.061	0.522
serum MG-H1 [ng/ml]	-0.063	0.511
serum CEL [ng/ml]	-0.124	0.195
serum CML [ng/ml]	-0.213*	0.025
serum Arg [µg/ml]	-0.128	0.180
serum Lys [µg/ml]	0.086	0.370

Regarding subcutaneous tissue density and advanced glycation end products in biofluids, we found a weak indirect correlation with serum Lys (Table 13). No other statistically significant differences were determined.

Table 13. Correlations between AGEs types in biofluids and subcutaneous tissue density.

Variable	SC TISSUE DENSITY N=111	
	r	p
plasma FruLys [µg/ml]	0.034	0.719
plasma Pyr [ng/ml]	-0.089	0.351
plasma MG-H1 [ng/ml]	-0.117	0.220
plasma CEL [ng/ml]	0.009	0.925
Plasma CML	-0.120	0.210
plasma Arg [µg/ml]	-0.117	0.220
plasma Lys [µg/ml]	-0.109	0.256
serum FruLys [µg/ml]	-0.160	0.093
serum Pyr [ng/ml]	-0.114	0.233
serum MG-H1 [ng/ml]	0.087	0.363
serum CEL [ng/ml]	0.746	0.746
serum CML [ng/ml]	0.049	0.606
serum Arg [µg/ml]	-0.075	0.434
serum Lys [µg/ml]	-0.191*	0.045

4. Discussion

The present cross-sectional study is the first to analyze the correlation between the accumulation of AGEs subtypes (CML, CEL, Arg, Pyr, MG-H1, FruLys, Lys) at the level of biofluids (plasma, serum, saliva, urine) and skin parameters of the AGEs cross-linking process by HFU (depth, density and degree of dermal pixelation). Pyr was isolated in 1849 by Anderson from the oil obtained by boiling animal bones at high temperatures, and years later its presence was found in volatile organic compounds produced by baking and preservation processes – fried chicken, roasted coffee, potato chips, fried ham, black tea [12–14]. In the present study, urinary Pyr and salivary MG-H1 values were lower in patients with cutaneous phenotype II compared to the others. Kostelc et al. found high values of Pyr at salivary level in patients with gingivitis, but related to the inflammatory component of its effects [15]. There are no other studies in the literature regarding AGEs in biofluids and facial phenotype, but it is known that Pyr induces capillary and skin depigmentation, which explains the low values in patients with facial phenotype II [16]. Compared to other biofluids, the lower MG-H1 concentration in saliva can be explained by the salivary composition in albumin, lysozyme, salivary amylase, which reacts to oxidative stress induced by the glycation phenomenon [17].

 doi:10.20944/preprints202602.2001.v1

Our study showed significant differences in urinary MG-H1, CEL and Arg concentrations, which were higher in female patients. Arg is a non-essential amino acid, with dietary origin and de novo synthesis (intestinal-renal axis) [18]. The literature attests that nitric oxide precursors and arginine methylation (function in ammonia assimilation in the uric cycle and its transformation into urea, creatinine, nitric oxide) together with MG with predominantly dietary origin, are biological markers of reduced glomerular filtration rate, and reduced renal glyoxalase-1 (Glo1) function [19–21].

The results of the present study did not bring significant differences between age groups and glycation end products at the level of biological fluids. The specialized literature contradicts our result, because carbonyl groups, oxidative stress, total thiol number, increase with age [22,23]. The justification of our result is represented by the age groups included in the study, which were close (40-60 years), which influenced the uniformity of AGEs values at the level of biofluids. We determined the existence of a weak direct correlation between MG-H1, from plasma and epidermal thickness, a weak indirect correlation between epidermal thickness and plasma Arg, CEL, the same salivary variables being in close correlation with epidermis density. There are no similar studies in the literature, but our results are in agreement with those of Christidis et al., who correlated reduced density and pixelation of the dermis (assessed by HFU) in sun-exposed areas, especially in patients with metabolic syndrome [24].

Regarding advanced glycation end products and the depth of the dermis affected by UV exposure, we established a weak positive correlation with serum Pyr, MG-H1, Arg, Lys, and salivary CML. Also, regarding the increased degree of pixelation of dermal collagen exposed to UV rays, it was directly related to MG-H1, salivary CML, and indirectly with the same products in urine. HFU reflects echogenic structural changes potentially associated with glycated collagen fibers in the dermis and connective tissue, where the degree of pixelation increases with a reduction in dermal elasticity, associated with the phenomenon of collagen glycation, which also indicates structural-functional tissue changes.

The changes revealed by HFU are in agreement with Monnier and Gkogkolou, who showed that the accumulation of AGEs and the fluorescence given by cross-linking are directly correlated with the loss of dermal elasticity and the increase in tissue autofluorescence [25,26]. Our study showed that, with the increase in the degree of damage to collagen by the glycation process in the skin exposed to UV rays, the serum values of glycation products (Arg, Lys, Pyr, CEL) are lower, which shows the capture of AGEs at the tissue level, in agreement with other studies that evaluated the accumulation of AGEs by autofluorescence [27–29].

Dermis aging was directly correlated with CML and salivary MG-H1, a promising aspect for the diagnosis and monitoring of the level of inflammation at a systemic level and, very importantly, of tissue aging. Both in the present study and in the specialized literature, the direct link between glycation of collagen fibers and systemic inflammatory markers was demonstrated [30–32]. It was also shown that the cross-linking phenomenon can be assessed by HFU and autofluorescence.

The assessment of HFU can be influenced by the facial phenotype, more specifically by the amount of melanin in the basal epidermal layers [33].. In the present study, most of the included subjects were part of phenotype III, and the exclusion criteria respected the absence of actinic erythema, skin hyperpigmentation formations or hyperkeratoses, which is why we considered that there was no possibility of inducing bias in the HFU results.

Our study is the first to demonstrate quantitative correlations between advanced glycation end products (CML, CEL, Arg, Pyr, MG-H1, FruLys, Lys) at the biofluid level (plasma, serum, saliva, urine) and skin parameters of the AGEs cross-linking process by HFU (dermal depth, density and degree of pixelation). Furthermore, the analysis in the four environments revealed a weak direct correlation between FruLys at plasma and serum levels, a weak indirect correlation with FruLys at salivary levels, a weak direct correlation between plasma and salivary MG-H1. results that provide a solid basis for AGEs quantification.

Regarding skin health, AGEs, and prevention, community health initiatives should prioritize dietary education on reducing sugar intake, and ultra-processed foods (high in dietary AGEs) to limit

 doi:10.20944/preprints202602.2001.v1

the endogenous production of glycation products and mitigate systemic inflammation. Also, as strict photoprotection measures, should promote rigorous "UV hygiene" protocols—including the daily use of broad-spectrum sunscreen and physical barriers, while advocate for the adoption of HFU of the skin in routine preventive check-ups; utilizing skin health as a readily accessible, as an accessible screening tool for identifying glycation-related cardiovascular risk.

As our study is an exploratory one, and, given the large number of correlations we performed, the results should be interpreted with caution and will require confirmation from independent cohorts.

5. Conclusions

HFU ultrasound assessment revealed structural changes in the cervico-facial dermis, which were associated with increased AGEs, suggesting that glycation-induced tissue remodeling can be detected non-invasively. This data obtained might be the based for future studies on the clinical utility of the combined assessment of AGEs and skin changes by HFU as modern, rapid and non-invasive tools with potential relevance for cardiometabolic risk research which require further studies.

Author Contributions: Conceptualization, A.M.B., S.C.V. and A.I.; methodology, C.F.; validation, A.M.B, O.S. and A.R.; formal analysis, S.C.V.; investigation, A.M.B., S.I.V.; data curation, A.E.M, S.C.V.; writing—original draft preparation, A.M.B, S.C.V., S.I.V. C.F.; writing—review and editing, A.I., O.S., A.R.; supervision, A.I.; All authors have read and agreed to the published version of the manuscript.

Funding: This research received no external funding.

Informed Consent Statement: Written informed consent has been obtained from the patients to publish this paper.

Conflicts of Interest: The authors declare no conflicts of interest.

Abbreviations

The following abbreviations are used in this manuscript:

AGEs - Advanced Glycation End Products

Arg - Arginine

CEL - Carboxy-ethyl-lysine

CML - Carboxy-methyl-lysine

CRP - C reactive protein

Fru-Lys- Fructose-lysine

HDL – C - High-density lipoprotein

HFU - High Frequency Ultrasound

IL 6 - Interleukin 6

MetS – Metabolic syndrome

MG-H1 - Methylglycoxal H1

Pyr - Pyridine

RAGE - AGE receptor

TNF α - Tumor necrosis factor alpha

Sc – subcutaneous tissue

UV – ultraviolet exposure

 doi:10.20944/preprints202602.2001.v1

References

1. Constitution of the World health organization. Definition of health, **2006**.
2. Balkau, B.; Charles, M.A.; Drivsholm, T.; Borch-Johnsen, K.; Wareham, N,; Yudkin, J.S.; Morris, R.; Zavaroni., I.; van Dam R.; Feskins, E.; Gabriel, R.; Diet, M.; Nilsson, P.; Hedblad, B.; European Group For The Study Of Insulin Resistance (EGIR). Frequency of the WHO metabolic syndrome in European cohorts, and an alternative definition of an insulin resistance syndrome. *Diabetes Metab* **2002** *Nov;28(5):* 364-76. PMID: 12461473.
3. Carrión-Barberà, I.; Triginer, L.; Tío, L.; Pérez-García, C.; Ribes, A.; Abad, V.; Pros, A.; Bermúdez-López, M.; Castro-Boqué, E.; Lecube, A.; Valdivielso, J.M.; Ilervas Project Group, Monfort, J.; Salman-Monte, T.C. Role of Advanced Glycation End Products as New Biomarkers in Systemic Lupus Erythematosus. *Int J Mol Sci* **2024** *Mar 5;25(5)*: 3022. doi: 10.3390/ijms25053022.
4. Israelsen, N.M.; Michael, M.; Mogensen, M.; Bojesen, S.; Jensen, M.; Hædersdal, M.; Podoleanu, A.; Bang, O. The value of ultrahigh resolution OCT in dermatology - delineating the dermo-epidermal junction, capillaries in the dermal papillae and vellus hairs. *Physics* **2018**, *arXiv*:1802.0145
5. Momma, H.; Niu, K.; Kobayashi, Y.; Guan, L.; Sato, M.; Guo, H.; Chujo, M.; Otomo, A.; Yufei, C.; Tadaura, H.; Saito, T.; Mori, T.; Miyata, T.; Nagatomi, R. Skin advanced glycation end-product accumulation is negatively associated with calcaneal osteo-sono assessment index among non-diabetic adult Japanese men. *Osteoporos Int* **2012** *Jun;23(6):* 1673-81. doi: 10.1007/s00198-011-1753-4. Epub 2011 Sep 8. PMID: 21901479
6. Chen, J.; Arshi, B.; Waqas, K.; Lu, T.; Bos, D.; Ikram, M.A.; Uitterlinden, A.G.; Kavousi, M.; Zillikens, M.C. Advanced glycation end products measured by skin autofluorescence and subclinical cardiovascular disease: the Rotterdam Study. *Cardiovasc Diabetol* **2023** *Nov 28;22(1):* 326. doi: 10.1186/s12933-023-02052-7.
7. Băbțan, A.M.; Vesa, Ș.C.; Boșca, B.A.; Crișan, M.; Mihu, C.M.; Băciuț, M.F.; Dinu, C.; Crișan, B.; Câmpian, R.S.; Feurdean, C.N.; Ionel, A.; Bezugly, A.; Bordea, I.R.; Ilea A. High-Frequency Ultrasound Assessment of Skin and Oral Mucosa in Metabolic Syndrome Patients-A Cross-Sectional Study. *J Clin Med* **2021** *Sep 28;10(19):* 4461. doi: 10.3390/jcm10194461. PMID: 34640479; PMCID: PMC8509493.
8. Alimova, S.; Sharobaro, V,\.; Yukhno, A. & Bondarenko, E. Possibilities of ultrasound examination in the assessment of age-related changes in the soft tissues of the face and neck: A review. *Appl Sci* **2023** https://doi.org/10.3390/app13021128
9. Machet, L et al. High resolution ultrasound imaging of melanocytic and other pigmented lesions of the skin. *Ultrasound Imaging* **2021, April** https://doi.org/10.5772/15372
10. Czajkowska, J.; Juszczyk, J.; Bugdol, M.N. et al. High-frequency ultrasound in anti-aging skin therapy monitoring. *Sci Rep* **2023** *13:* 17799. https://doi.org/10.1038/s41598-023-45126-y
11. Anderson, T. (1849). *"Producte der trocknen Destillation thierischer Materien"* [Products of the dry distillation of animal matter]. Annalen der Chemie und Pharmacie (in German). 2020; 70:32–38. doi:10.1002/jlac.18490700105
12. Aeschbacher, H.U.; Wolleb, U.; Löliger, J.; Spadone, J.C.; Liardon, R. Contribution of coffee aroma constituents to the mutagenicity of coffee". *Food and Chemical Toxicology* **1989** *27(4):* 227–232. doi:10.1016/0278-6915(89)90160-9.
13. Buttery, R.G.; Seifert, R.M.; Guadagni, D.G.; Ling, L.C. Characterization of Volatile Pyrazine and Pyridine Components of Potato Chips. *Journal of Agricultural and Food Chemistry* **1971** *19 (5).* Washington, DC: ACS: 969–971.
14. Ho, C.T.; Lee, K.N.; Jin, Q.Z. Isolation and identification of volatile flavor compounds in fried bacon. *Journal of Agricultural and Food Chemistry* **1983** *31(2):* 336. doi:10.1021/jf00116a038.
15. Kostelc, J.G.; Preti, G.; Nelson, P.R.; Brauner, L.; Baehni, P. Oral Odors in Early Experimental Gingivitis". *Journal of Periodontal Research* **1984** *19(3):* 303–312.doi:10.1111/j.1600-0765.1984.tb00821.x.
16. Muraoka, M.Y.; Justino, A.B.; Caixeta, D.C.; Queiroz, J.S.; Sabino-Silva, R.;, Salmen Espindola F. Fructose and methylglyoxal-induced glycation alters structural and functional properties of salivary proteins, albumin and lysozyme. *PLoS One* **2022** *Jan 21;17(1):* e0262369. doi: 10.1371/journal.pone.0262369. PMID: 35061788; PMCID: PMC8782344.
17. Morris, S.ML Jr. Arginine Metabolism Revisited. *J Nutr* **2016** *Dec;146(12):* 2579S-2586S. doi: 10.3945/jn.115.226621

 doi:10.20944/preprints202602.2001.v1

18. Kleinebenne, L.; Röhrig, W,; Ebach, F.; Reutter, H.; Pankraz, A.; Heuchel, K.M.; Müller, A.; Hilger, A.C. The components of arginine and methylarginine metabolism are indicative of altered kidney function in intrauterine growth-restricted neonates. *J Hypertens* **2024** *Nov 1;42(11):* 1940-1947. doi: 10.1097/HJH.0000000000003818.
19. Emrich, I.E.; Zawada, A.M.; Martens-Lobenhoffer, J.; Fliser, D.; Wagenpfeil, S.; Heine, GH.; Bode-Boger, S.M. Symmetric dimethylarginine (SDMA) outperforms asymmetric dimethylarginine (ADMA) and other methylarginines as predictor of renal and cardiovascular outcome in nondialysis chronic kidney disease. *Clin Res Cardiol* **2018** *107:* 201–213.
20. Rabbani, N.; Thornalley, P.J. Advanced glycation end products in the pathogenesis of chronic kidney disease. *Kidney Int* **2018** *Apr;93(4):* 803-813. doi: 10.1016/j.kint.2017.11.034.
21. Kaleta, D.; Polańska, K.; Korytkowski, P.; Usidame, B.; Bąk-Romaniszyn, L. Patterns of nicotine dependence in four Eastern European countries. *BMC* Public Health **2015** *Nov 28;15:* 1189. doi: 10.1186/s12889-015-2537-0.
22. Maciejczyk, M.; Nesterowicz, M.; Szulimowska, J.; Zalewska, A. Oxidation, Glycation, and Carbamylation of Salivary Biomolecules in Healthy Children, Adults, and the Elderly: Can Saliva Be Used in the Assessment of Aging? *J Inflamm Res* **2022** *Mar 28;15:* 2051-2073. doi: 10.2147/JIR.S356029.
23. Maciejczyk, M.; Bielas, M.; Zalewska, A.; Gerreth, K. Salivary Biomarkers of Oxidative Stress and Inflammation in Stroke Patients: from Basic Research to Clinical Practice. *Oxid Med Cell Longev* **2021** 2021:5545330. doi: 10.1155/2021/5545330
24. Christidis, G.; Küppers, F.; Karatayli, S.C. et al. Skin advanced glycation end-products as indicators of the metabolic profile in diabetes mellitus: correlations with glycemic control, liver phenotypes and metabolic biomarkers. *BMC Endocr Disord* **2024** *24*: 31. https://doi.org/10.1186/s12902-024-01558-9
25. Monnier, V.M.; Sun, W.; Gao, X.; Sell, D.R.; Cleary, P.A.; Lachin, J.M. et al. Skin collagen advanced glycation endproducts (AGEs) and the long-term progression of subclinical cardiovascular disease. *Diabetes Care* **2015** *38(7):* 1170-75.
26. Gkogkolou, P.; Böhm M. Advanced glycation end products: Key players in skin aging? *Dermatoendocrinol* **2012** *4(3):* 259-70 https://doi.org/10.4161/derm.22028
27. Du, T.; Brandl, B.; Hauner, H.; & Skurk, T. Skin Autofluorescence Mirrors Surrogate Parameters of Vascular Aging: An Enable Study. *Nutrients* **2023** *15(7):* 1597. https://doi.org/10.3390/nu15071597
28. Meerwaldt, R.; Hartog, J.W.; Graaff, R.; Huisman, R.J.; Links, T.P.; den Hollander, N.C. et al. Skin autofluorescence, a measure of cumulative metabolic stress and advanced glycation end products, predicts mortality in hemodialysis patients. *J Am Soc Nephrol* **2005** *6(12):* 3687-93 doi: 10.1681/ASN.2005020144.
29. Petrofsky, J.S.; Lee, S.; Hamdan, T. et al. High-frequency ultrasound analysis of skin structure and its relation to glycation. *J Clin Med* **2021** *10(19):* 4461.
30. Saremi, A.; Howell, S.; Schwenke, D.C.; Bahn, G.; Beisswenger, P.J; Reaven, P.D. for the VADT Investigators. Advanced Glycation End Products, Oxidation Products, and the Extent of Atherosclerosis During the VA Diabetes Trial and Follow-up Study. *Diabetes Care* **2017** *1 April 40(4):* 591–598. https://doi.org/10.2337/dc16-1875
31. Zhao, X.W.; Yue, W.X.; Zhang, S.W.; Chen, Q. Correlation between the accumulation of skin glycosylation end products and the development of type 2 diabetic peripheral neuropathy. *BMC Endocr Disord* **2022** *22(1):* 106.

 doi:10.20944/preprints202602.2001.v1

32. Reurean-Pintilei, D.; Stoian, A.P.; Potcovaru, C.G. et al. Skin autofluorescence as a potential adjunctive marker for cardiovascular risk assessment in type 2 diabetes: A systematic review. *Int J Mol Sci* **2024** *25(7):* 3889.
33. Martinovic, D.; Tokic, D.; Usljebrka, M.; Lupi-Ferandin, S.; Cigic, L.; Vanjaka Rogosic, L.; Ercegovic, S.; Kontic, M.; Kumrić, M.; Rusic, D.; Vilovic, M.; Leskur, M.; Bozic, J. The Association between the Level of Advanced Glycation End Products and Objective Skin Quality Parameters. *Life (Basel)* **2023** *Jan 17;13(2):* 256. doi: 10.3390/life13020256.